

# A multi-proxy reconstruction of spatial and temporal variations in Asian summer temperatures over the last millennium

Feng Shi<sup>1</sup> · Quansheng Ge<sup>2</sup> · Bao Yang<sup>3</sup> ·  
Jianping Li<sup>4,5</sup> · Fengmei Yang<sup>6</sup> ·  
Fredrik Charpentier Ljungqvist<sup>7,8</sup> · Olga Solomina<sup>9,10</sup> ·  
Takeshi Nakatsuka<sup>11</sup> · Ninglian Wang<sup>3</sup> · Sen Zhao<sup>12</sup> ·  
Chenxi Xu<sup>11</sup> · Keyan Fang<sup>13</sup> · Masaki Sano<sup>11</sup> ·  
Guoqiang Chu<sup>1</sup> · Zexin Fan<sup>14</sup> · Narayan P. Gaire<sup>15,16</sup> ·  
Muhammad Usama Zafar<sup>17</sup>

Received: 1 August 2014 / Accepted: 18 April 2015 / Published online: 9 May 2015  
© Springer Science+Business Media Dordrecht 2015

**Abstract** To investigate climate variability in Asia during the last millennium, the spatial and temporal evolution of summer (June–July–August; JJA) temperature in eastern and south-central Asia is reconstructed using multi-proxy records and the regularized expectation maximization (RegEM) algorithm with truncated total least squares (TTLS), under a point-by-point regression (PPR) framework. The temperature index reconstructions show that the late 20th century was the

---

**Electronic supplementary material** The online version of this article (doi:10.1007/s10584-015-1413-3) contains supplementary material, which is available to authorized users.

✉ Quansheng Ge  
geqs@igsnr.ac.cn

- <sup>1</sup> Key Laboratory of Cenozoic Geology and Environment, Institute of Geology and Geophysics, Chinese Academy of Sciences, Beijing, China
- <sup>2</sup> Institute of Geographic Sciences and Natural Resources Research, Chinese Academy of Sciences, Beijing, China
- <sup>3</sup> Cold and Arid Regions Environmental and Engineering Research Institute, Chinese Academy of Sciences, Lanzhou, China
- <sup>4</sup> College of Global Change and Earth System Science, Beijing Normal University, Beijing, China
- <sup>5</sup> Joint Center for Global Change Studies, Beijing, China
- <sup>6</sup> China Meteorological Administration Training Centre, Beijing, China
- <sup>7</sup> Department of History, Stockholm University, Stockholm, Sweden
- <sup>8</sup> Bolin Centre for Climate Research, Stockholm University, Stockholm, Sweden
- <sup>9</sup> Institute of Geography, Russian Academy of Sciences, Moscow, Russia

warmest period in Asia over the past millennium. The temperature field reconstructions illustrate that temperatures in central, eastern, and southern China during the 11th and 13th centuries, and in western Asia during the 12th century, were significantly higher than those in other regions, and comparable to levels in the 20th century. Except for the most recent warming, all identified warm events showed distinct regional expressions and none were uniform over the entire reconstruction area. The main finding of the study is that spatial temperature patterns have, on centennial time-scales, varied greatly over the last millennium. Moreover, seven climate model simulations, from the Coupled Model Intercomparison Project Phase 5 (CMIP5), over the same region of Asia, are all consistent with the temperature index reconstruction at the 99 % confidence level. Only spatial temperature patterns extracted as the first empirical orthogonal function (EOF) from the GISS-E2-R and MPI-ESM-P model simulations are significant and consistent with the temperature field reconstruction over the past millennium in Asia at the 90 % confidence level. This indicates that both the reconstruction and the simulations depict the temporal climate variability well over the past millennium. However, the spatial simulation or reconstruction capability of climate variability over the past millennium could be still limited. For reconstruction, some grid points do not pass validation tests and reveal the need for more proxies with high temporal resolution, accurate dating, and sensitive temperature signals, especially in central Asia and before AD 1400.

## 1 Introduction

Temperature reconstructions of the last millennium are essential for a deeper understanding of natural climate variability before the beginning of instrumental records and the distinction of the anthropogenic and natural causes of temperature change (Jones et al. 1998). In recent years, some improvements in model simulations and reconstructions of hemispheric and global mean temperature trends and variability over the past millennium have been achieved (Masson-Delmotte et al. 2013). However, considerable uncertainties remain in the understanding of regional responses to large-scale changes in temperature (PAGES 2k Consortium 2013). Reconstructions of the spatial and temporal patterns of regional temperature variability are important for a better understanding and quantification of the influence of different external forces and internal feedbacks of the global climate system at scales that are most relevant to human society. However, in many parts of the world, data on patterns of past temperature variability are sparse, on account of a paucity of proxy record. To solve this problem the international Past Global Changes (PAGES) project established the PAGES 2k Network in 2009 (Newman et al. 2009). This network includes the Asia 2k group, which mobilized the

<sup>10</sup> Tomsk State University, Tomsk, Russia

<sup>11</sup> Research Institute for Humanity and Nature, Kyoto, Japan

<sup>12</sup> State Key Laboratory of Numerical Modeling for Atmospheric Sciences and Geophysical Fluid Dynamics, Institute of Atmospheric Physics, Chinese Academy of Sciences, Beijing, China

<sup>13</sup> Key Laboratory of Humid Subtropical Eco-Geographical Process (Ministry of Education), Fujian Normal University, Fuzhou, China

<sup>14</sup> Xishuangbanna Tropical Botanical Garden, Chinese Academy of Sciences, Yunnan, China

<sup>15</sup> Faculty of Science, Nepal Academy of Science and Technology, Khumaltar, Lalitpur, Nepal

<sup>16</sup> Central Department of Environmental Science, Tribhuvan University, Kirtipur, Kathmandu, Nepal

<sup>17</sup> Laboratory of Dendrochronology and Plant Ecology, Federal Urdu University, Gulshan-e-Iqbal Campus, Karachi, Pakistan

scientific community in Asia to obtain numerous proxy records that were not available from public data repositories, and then, produced temperature reconstructions and analyzed the spatial and temporal variability of reconstructed temperatures in Asia in the Common Era. From this initiative, Cook et al. (2013) presented the first Asian temperature field reconstruction, based on 229 tree-ring chronologies, which are now available from the World Data Center for Paleoclimatology ([https://www.ncdc.noaa.gov/cdo/f?p=519:7:::::P1\\_STUDY\\_ID,P1\\_SCIENCE\\_KEYWORD\\_ID:12712,82](https://www.ncdc.noaa.gov/cdo/f?p=519:7:::::P1_STUDY_ID,P1_SCIENCE_KEYWORD_ID:12712,82)). However, this temperature reconstruction is based only on tree-ring data and so any underlying low-frequency variability may not be well represented (Cook et al. 2013). Moreover, the number of tree-ring chronologies from eastern China is still too limited to accurately describe climate variations there (Yang et al. 2013).

To overcome these limitations, simultaneously another multi-proxy reconstruction project was launched. A multi-proxy approach, combining several types of natural archives as well as historical documentary data from eastern China, is here used to reassess and complement the first Asia2k tree-ring reconstruction by Cook et al. (2013). The new reconstruction provides an alternative assessment of past temperature change in Asia, and was used to identify which models that match the reconstructed temperature variability in Asia best.

## 2 Data and methods

### 2.1 Instrumental data

The Climatic Research Unit  $5 \times 5^\circ$  gridded instrumental surface air temperature dataset (CRUTEM4v) for the period AD 1920–1999 (Norwich, UK; [www.cru.uea.ac.uk/cru/data/temperature](http://www.cru.uea.ac.uk/cru/data/temperature); Jones et al. 2012) was used in this study. Based on the spatial distribution of available proxy records, the reconstructed area of eastern and south-central Asia was here defined as the area bounded by  $0^\circ\text{N}$ – $60^\circ\text{N}$  and  $60^\circ\text{E}$ – $145^\circ\text{E}$ . Instrumental data between AD 1920 and 1999 is lacking in four of the land grid cells centered at  $117.5^\circ\text{E}$ ,  $2.5^\circ\text{N}$ ;  $92.5^\circ\text{E}$ ,  $17.5^\circ\text{N}$ ;  $82.5^\circ\text{E}$ ,  $37.5^\circ\text{N}$ ;  $117.5^\circ\text{E}$ ,  $42.5^\circ\text{N}$ ; these areas were excluded from the reconstructions (Fig. S1). Thus, the 132 remaining grid cells were used to represent the land area of Asia (Fig. S1). The number of grid points possessing values in each year is shown in Fig. S2. More details of the rationales and selection process for the instrumental data used in this analysis are given in the [Supplementary material](#).

### 2.2 Temperature proxy data

The selection of proxy records for Asia was based on three criteria: 1) the candidate records were required to cover at least the period AD 1800–1975; 2) the non-tree-ring records were required to be sensitive to temperature change according to the original publication, and to have a temporal resolution of 30 years or less; and 3) the sampling density for the tree-ring chronologies was required to be four samples per year or more, and to show a positive relationship with temperature. The selection process for proxy records is explained in detail in the [Supplementary material](#).

Through a screening procedure, two groups of records were identified: A) all 418 available Asian proxy records, including those with restricted access (Fig. S3a); and B) only the 357 records publicly available from the World Data Centre for Paleoclimatology (Fig. S3b). All

records with restricted access have been published and described in peer-reviewed literature, and were derived from data repositories in Chinese research institutes, or provided by the original authors. Tables S1 and S2 provide further information on the dataset, including references to the original work, site, species, temporal resolution, geographic coordinates, and time period covered by the record.

### 2.3 Reconstruction method

Reconstructions based on the point-by-point regression (PPR) framework requires only proxy records that are close to or adjacent to, reconstruction grid points (Cook et al. 1999): because of this, these reconstructions retain regional information better than those based on frameworks that use only the first several principal components of the instrumental data (Mann et al. 2007). This is especially important for the Asian region, because the regional climate of Asia was strongly influenced by local factors, which thus affects the stability of climatic teleconnections (e.g. the Tibetan Plateau and the complex monsoon system) (Wu et al. 2012). In this study, a modified PPR framework was used, which is described below. The basis for the selection of the framework, and a more complete description of interpretation methods, are provided in the [Supplementary material](#).

#### Step 1: Processing proxy data

Firstly, records were standardized, with respect to the common period AD 1800–1975. Values that exceeded five standard deviations of the variation observed during the period AD 1800–1975 were considered as outliers. If the number of outliers was more than 10 % of the length of the record, then that record was excluded. All outliers were otherwise reassigned by linear interpolation. Secondly, proxy records with a resolution of less than 1 year were interpolated to annual resolution using a cubic spline function. Finally, proxy records lacking data during the period AD 1976–1999 were extrapolated, using the RegEM algorithm with ridge regression method (Schneider 2001), based on mutual covariance calculated between the remaining data and other available proxy records for the period AD 1800–1999. The parameters used for the interpolation were the same as those in Mann et al. (2008). For group A, 220 of the 418 (52.6 %) records were extrapolated to AD 1999 with the mean length of extrapolation being 6 years. For group B, 179 of the 357 (50.1 %) records were extrapolated to AD 1999 with the mean extrapolation being 5 years.

#### Step 2: Splitting proxy and instrumental data

The majority of the records used for the reconstruction was comprised of tree-ring data, for which extraction of low-frequency information is often more difficult than for other proxies (Moberg et al. 2005). This potential reduction in the low-frequency signal is due to the effect of the ‘segment length curse’ (Cook et al. 1995), which states that the preservation of cycle signals longer than the length of individual tree-ring samples is difficult to achieve. However, other types of proxy records often have less than annual resolution and may contain dating uncertainties. Therefore, the proxy records and instrumental data were all filtered through a Butterworth IIR filter with a  $0.1 \text{ year}^{-1}$  cut-off frequency, and only the low-frequency band of past temperature was reconstructed.

#### Step 3: Regressing proxy record

The RegEM algorithm is a sophisticated method used in paleoclimate reconstructions (Guiot et al. 2010; Mann et al. 2008; Wang et al. 2014; Neukom et al. 2011) to

build a transfer function. We used the PPR to locate predictor proxies, which is important for the Asian region, due to its complex topography and heterogeneous climate. On the other hand, a larger search radius allows the inclusion of more proxy records as predictors, ensuring the reliability and consistency of results at adjacent grid points. In this study, all grid cells were reconstructed using proxy data from within either one or two adjacent cells. A PPR search radius of 746–1389 km was retained as the most practical option.

#### Step 4: Validating reconstructions

The accuracy of the reconstruction for each grid-point was evaluated using a split-period approach (Mann et al. 2008). The instrumental data were split into two parts (AD 1920–1959 and AD 1960–1999), which were alternatively used as calibration and validation periods. The reconstruction skill was measured using the Reduction of Error (RE) and the Coefficient of Efficiency (CE), and the computer code from Mann et al. (2008). The final verification results were the average of the verification results from the two calibration processes.

The statistical tests may provide results with only limited value for assessing the quality of the record over the instrumental period, not the full reconstruction period. As such, the reconstruction in this paper is also compared with the independent data from the last millennium (AD 850–1849), derived from experiments of seven climate model simulations from CMIP5, in both the spatial and temporal domain (Schmidt et al. 2012). Table S3 shows the details of the seven models, which include the BCC-CSM1.1 (Wu et al. 2010), CCSM4 (Landrum et al. 2013), FGOALS-s2 (Man and Zhou 2014), GISS-E2-R (Schmidt et al. 2014), HadCM3 (Schurer et al. 2013), IPSL-CM5A-LR (Dufresne et al. 2013) and MPI-ESM-P (Jungclaus et al. 2010) (see the [Supplementary material](#) for more information on these models). All simulation results were interpolated to the same temporal and spatial resolution, and were assessed over the same area and time period as the reconstruction in this study.

## 3 Results and discussion

### 3.1 Index reconstructions

The reconstruction provides robust measures of past temperature changes over most of Asia, in areas of positive RE and CE values (Fig. S4). Details of the verification results are shown in the [Supplementary material](#). There is a small difference between the two versions of reconstructed temperature anomalies (A and B) with respect to AD 1961–1990 over the past 1100 years in Asia (see Fig. 1a; Fig. S5). The amplitude of the temperature variability in version A, which is derived from all proxy records, is more strongly expressed than in version B. Distinct periods identified in the temperature index reconstructions, include the Medieval Climate Anomaly (MCA; also known as the Medieval Warm Period), the Little Ice Age (LIA) and the late 20th century warming. Here, the MCA and LIA are defined as AD 950–1250 and AD 1400–1700, respectively, following the definitions of Mann et al. (2009). During the past millennium, the late 20th century was the warmest period, and the 16th and 17th centuries were the two coldest periods in the reconstruction.

After AD 1950, the reconstructed temperatures differ markedly from those of Mann et al. (2009) and Cook et al. (2013) (Fig. 1b). The amplitudes of the reconstructed temperatures in

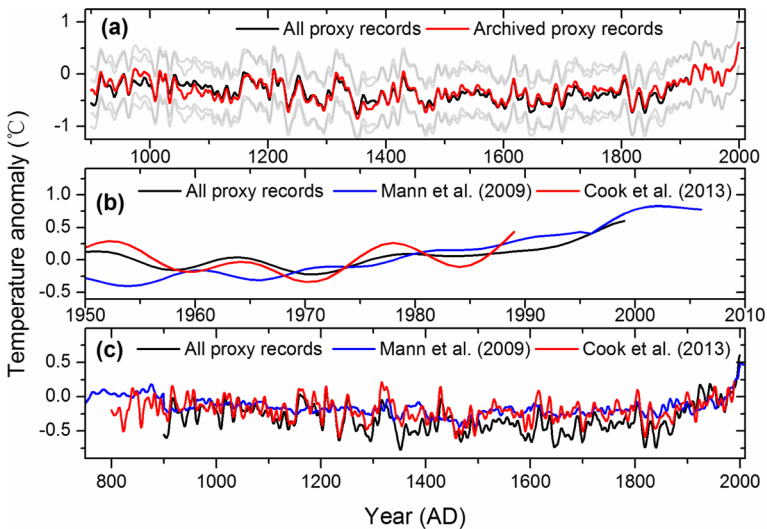


**Fig. 1** **a** Reconstructed temperature anomalies (with respect to AD 1961–1990) for Asia over the last millennium using all proxy records (version A; *black line*) and using publicly available proxy records only (version B; *red line*), including their uncertainties ( $\pm 2$  times the residual standard deviation; *gray lines*). **b** comparison of the original sequences of version A reconstruction (*black line*), the reconstruction of Mann et al. (2009) (*blue line*) and the reconstruction of Cook et al. (2013) (*red line*) between AD 1950 and 2000; and **c** versions of the three reconstructions with variance matched to that of instrumental data (CRUTEM4v) for AD 1951–1989

Mann et al. (2009) and Cook et al. (2013) both are significantly smaller than that of the present study (in Fig. 1c); the standard deviations over the period AD 900–1989 were 0.09, 0.15, and 0.19 for Mann et al. (2009), Cook et al. (2013), and this study, respectively. The lower standard deviation of the reconstruction by Mann et al. (2009) was probably caused by the averaging of a limited number of less well correlated proxy records over most of Asia. Some records in the reconstruction by Mann et al. (2009) (e.g. Zhang 1980; Wang and Wang 1990) have been updated to higher-resolution and higher-quality versions (e.g. Wang et al. 2007; Ge et al. 2010), and these updated records were used in this study.

The present reconstruction shows a relatively distinct LIA, as compared with the reconstruction of Cook et al. (2013) (Fig. S6), and it is not surprising, as tree-ring chronologies sometimes show lower amplitudes and less low-frequency variation than do multi-proxy reconstructions (Moberg et al. 2005). The present study included other no-tree-ring proxy records, and these records may contain a relatively higher proportion of low-frequency signals: e.g. this study includes eight historical document records from eastern China. Climatic variability in eastern and western China at least some of the last millennium was probably asynchronous (Ge et al. 2013; Shi et al. 2012). Thus, it is necessary to include the non-tree-ring proxy records to obtain a more comprehensive signal of regional climate variability.

### 3.2 Field reconstructions

In this study the spatial patterns of regionally averaged summer temperature anomalies (with respect to AD 1961–1990) in Asia over the last millennium are more coherent in version A (Fig. 2a) than in version B of the reconstruction (Fig. S7), because of the denser proxy coverage in version A. In addition, version A shows a distinct warm period over most of China in the 13th

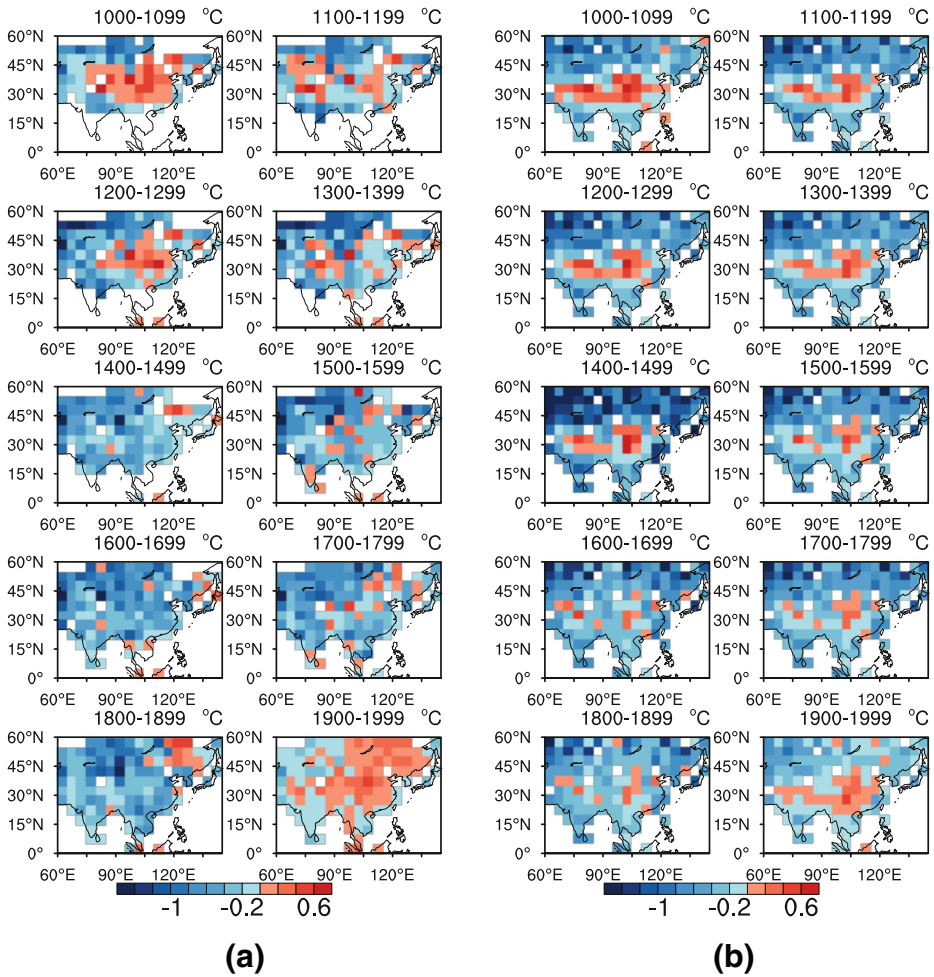


**Fig. 2** Spatial patterns of summer temperature anomalies in Asia over the last millennium from the 11th to 20th centuries, with respect to AD 1961–1990, **a** for the version A reconstruction, and **b** for the reconstruction by Mann et al. (2009)

century (Fig. 2a), especially in central and eastern China, but this warm period does not appear in version B (Fig. S7). Previous temperature reconstructions for China also show a warm period at this time (Ge et al. 2013), similar to that of version A in our reconstruction. Both reconstructions from the present study show three other warm periods in the 11th, 12th, and 20th centuries, although the spatial patterns presented by the two versions for the first two warm periods are a little different to one another. Both versions show that temperatures in central, southern and eastern China in the 11th century were significantly higher than in other parts of Asia, whereas in central Asia, temperatures were distinctly higher during the 12th century. These patterns contrast with the warming in the 20th century, which portray strong east–west temperature gradients and a uniform warming trend over most of Asia. It should be noted that in some regions, high temperatures during the warm periods of the 11th, 12th and 13th centuries were comparable with those of the late 20th century. After the MCA, in the 14th century, temperatures in Asia

started to decrease, and reached their minimum values in most regions in the 17th century. This minimum corresponds to the peak of the LIA as observed in most of the Northern Hemisphere (see, e.g., Ljungqvist et al. 2012; PAGES 2k Consortium 2013). The cold event of the 17th century was spatially uniform over most of the Asian region. The warming that occurred after the LIA was spatially less coherent, as during the 20th century, the eastern Asian regions became distinctly warmer than those in the west. This indicates spatially heterogeneous expressions of temperature patterns over Asia during warm periods. Whether spatial variations during the MCA represent true regional signals or is a reconstruction artifact requires verification, as the number of proxy records covering this period limited.

The spatial pattern in the temperature reconstruction of Mann et al. (2009) (Fig. 2b), differed notably to that of the field reconstruction in the present study, for the same area and time period (Fig. 2a). In particular, in their reconstruction, the shape of warming is relatively consistent during the 12th, 13th, and 14th centuries, and is similar to that of the 20th century. However, only a small number of cells in the reconstruction of Mann et al. (2009) passed the validation tests, probably because of the sparser proxy data coverage in their reconstruction as compared with that used in the present reconstruction. Thus, substantial progress has been achieved since previous global climate field reconstructions, which were limited in their ability to accurately reproduce regional climate variability in Asia (Figs. 1c and 2b).

### 3.3 Comparison with climate model simulations

Version A of the temperature reconstruction reproduces the orbital forced cooling trend and the centennial summer temperature variations in Asia similar to those of the seven different climate model simulations (at the 99 % confidence level) based on 11-year moving averages during the common period AD 900–1849 (Fig. 3). The significance of the correlations has been verified using the effective number of degrees of freedom (Li et al. 2013). The GISS-E2-R and HadCM3 models follow the reconstruction especially well and exhibit the highest correlation coefficients of all seven models with the reconstruction (0.59 and 0.52, respectively; both significant at the 99 % confidence level). The HadCM3 also reproduces decadal variations in the reconstruction reasonably well. All of the simulations show strong cooling in response to one of the largest eruption of a tropical volcano in the past millennium in AD 1258–1259 (Timmreck et al. 2009); however, this signal is not recorded in the index reconstruction. Whether natural proxy records (such as tree-ring width) can fully capture cooling signals driven by volcanic eruptions has been debated recently in the scientific literature (Anchukaitis et al. 2012; Mann et al. 2012), although Esper et al. (2013) showed that, at least in Europe, tree-ring data can capture the post-volcanic cooling observed in early instrumental data. The temperature reconstruction in this study suggests that the AD 1258–1259 volcanic eruption did not have a large impact on Asian temperatures, as indicated by the models. The absence of a volcanic eruption effect on climate in Asia is supported by the historical documentary data from China, which indicate that the entire middle Nan Song dynasty (AD 1201–1270) was relatively warm (Ge et al. 2013).

EOF analysis of averaged summer (JJA) temperature anomalies for the version A reconstruction, and of the model simulations, during the common period AD 900–1849, suggest that the pattern of the first EOF (EOF1) of the reconstruction reflects heavily temperature loadings over western Asia, with less loadings over the central and eastern Asia region (Fig. 4). The



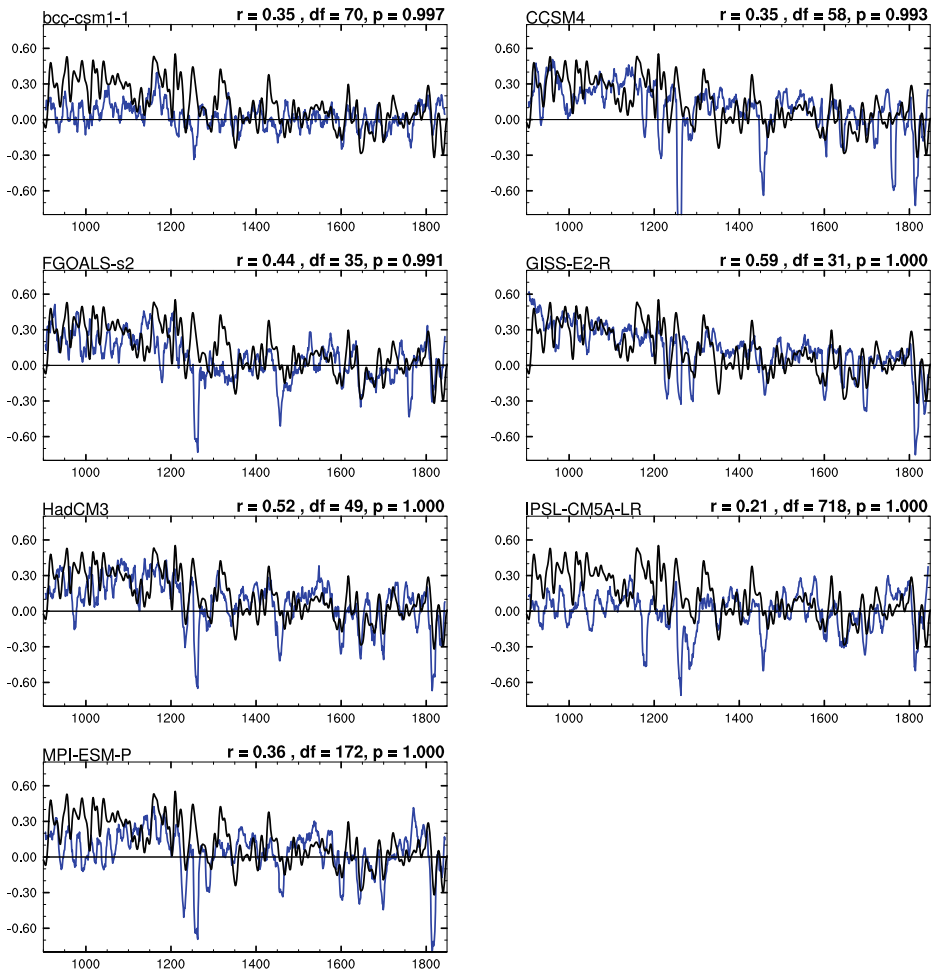


**Fig. 3** Comparison of version A of the temperature reconstruction for Asia (*black line*) and the seven climate model simulations for Asia over the past millennium (*blue lines*), with respect to AD 1500–1849

EOF1 of the reconstruction explains 26.8 % of the total variance, and the EOF1 of each of five of the seven model simulations explains all more than 40 % of the total variance. The best simulations of the reconstructed spatial pattern of temperature in Asia is provided by the MPI-ESM-P and GISS-E2-R models (correlation coefficients between the EOF1 spatial pattern of the simulation and reconstruction are 0.66 and 0.59, respectively). However, all the remaining five models showed positively loadings over most of the domain, except for the above two models, and, did not consistently simulate spatial patterns as revealed by the reconstruction. The EOF1 time series of three climate models (GISS-E2-R, HadCM3 and MPI-ESM-P) also correlate with the reconstruction of this study at the 90 % confidence level (correlation coefficients of 0.35, 0.35 and 0.27, respectively). The EOF1 time series show distinct trends, with a negative phase representing a cold west and warm east pattern before AD 1400, and a positive phase showing the opposite pattern after AD 1400. This indicates that the MPI-ESM-

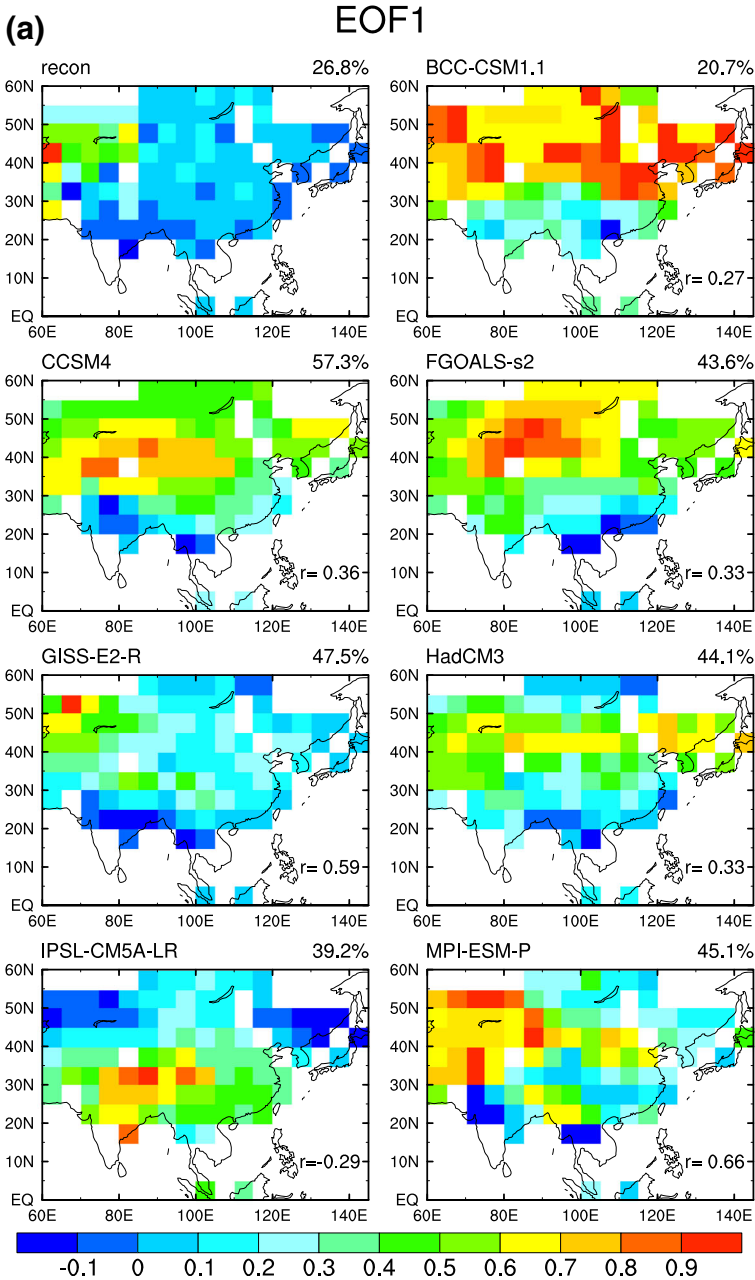


**Fig. 4** Spatial patterns of Empirical orthogonal function (EOF) analysis of the temperature anomalies of the version A temperature reconstruction and the seven climate model simulations, for Asia over the past millennium, with respect to AD 1500–1849. **a** Spatial patterns, and **b** time-series

P and GISS-E2-R models may more accurately simulate the spatial patterns of temperature variations in Asia for the period AD 900–1849 than the other five models.

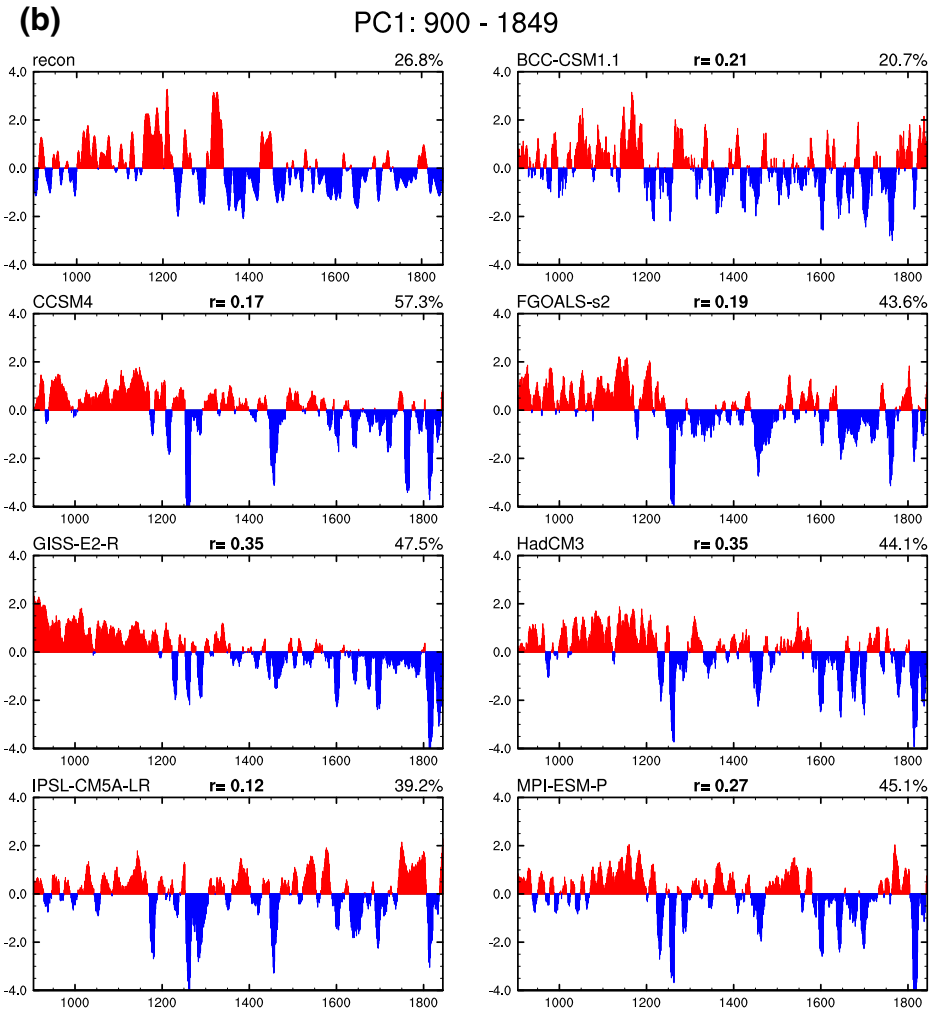


Fig. 4 continued

## 4 Conclusions

We have reconstructed spatial and temporal patterns of temperature in Asia over the past millennium using two different proxy datasets: one that includes and one that excludes proxy records that are not publicly available (versions A and B, respectively). These datasets produced two similar temperature index reconstructions for Asia, both of which retain more low-frequency signals than the previously published tree-ring reconstruction of Cook et al. (2013). The two temperature index reconstructions both show that the late 20th century was probably the warmest period over most of Asia during the past millennium.

This is the first spatial field multi-proxy temperature reconstruction for Asia over the past millennium. Prominent features of the reconstruction include the warm periods in the 11th and 13th centuries and a cold period in the 17th century. Reconstructed temperatures for central, eastern and

southern China during the 11th and 13th centuries, and for western Asia during the 12th century, were significantly higher than for other regions, and were comparable with those of the 20th century. All identified warm events showed distinct regional expressions. The spatial pattern during the LIA was uniform over the entire area of the reconstruction. It suggests that the spatial coherence of the temperature anomaly pattern has varied with time over the last millennium in Asia. However, the low reconstruction skill in some grid cells indicates the fact that the number of proxy records needed to reconstruct the spatial temperature field in some parts of central Asia is insufficient; proxy data are particularly scarce for these regions prior to c. AD 1400.

The temperature index reconstruction correlates well with seven different climate model simulations at the 99 % confidence level. Moreover, the HadCM3 model even reproduces consistent temperature reconstruction variations at decadal time-scales. Spatially, both the GISS-E2-R and MPI-ESM-P models show patterns similar to those of the spatial field reconstructions from this study for the common period AD 900–1849. This indicates that those two models could more accurately simulate the main features of the spatial pattern of the first EOF of summer temperature during the past millennium over Asia than the other models. The present temperature field reconstruction will help to improve our understanding of the influence of external forces (orbital changes, solar activity, volcanic eruptions and greenhouse gases) and oceanic internal variability on local scale climate dynamics.

**Acknowledgments** Version B of the reconstruction is a contribution to the PAGES Asia2k working group. We are indebted to Lucien von Gunten for helpful comments and assistance, and thank Edward R. Cook, Brendan Buckley, Kevin Anchukaitis, Paul J. Krusic, Chun Qin, Xuemei Shao, Jingyun Zheng, Hemant Borgaonkar, Katsuhiko Kimura, Masumi Zaiki, Koh Yasue, Achim Bräuning, Jiangfeng Li, Yujiang Yuan, Hongbing Liu, Yu Liu, Qibing Zhang, Jinbao Li, Jianfeng Peng, Xiaohua Gou, Haifeng Zhu, Shaowu Wang, Deer Zhang, Jonathan Palmer, Paul Sheppard, Margit Schwikowski, Tatyana Papina and other scientists who have contributed their proxy data for the study region to the publicly available database. The study was jointly funded by the CAS Strategic Priority Research Program Grant (XDA05080800; XDB03020500), and the National Natural Science Foundation of China (41301220). Feng Shi was supported by China Meteorological Administration Drought Research (IAM201213) and West Light Program for Talent Cultivation of Chinese Academy of Sciences.

## References

- Anchukaitis KJ, Breitenmoser P, Briffa KR, Buchwal A, Büntgen U, Cook ER, D'Arrigo RD, Esper J, Evans MN, Frank D, Grudd H, Gunnarson BE, Hughes MK, Kirilyanov AV, Korner C, Krusic PJ, Luckman B, Melvin TM, Salzer MW, Shashkin AV, Timmreck C, Vaganov EA, Wilson RJS (2012) Tree rings and volcanic cooling. *Nat Geosci* 5:836–837
- Cook ER, Briffa KR, Meko DM, Graybill DA, Funkhouser G (1995) The 'segment length curse' in long tree-ring chronology development for palaeoclimatic studies. *The Holocene* 5(2):229–237
- Cook ER, Meko DM, Stahle DW, Cleaveland MK (1999) Drought reconstructions for the continental United States. *J Clim* 12(4):1145–1162
- Cook ER, Krusic PJ, Anchukaitis KJ, Buckley BM, Nakatsuka T, Sano M (2013) Tree-ring reconstructed summer temperature anomalies for temperate East Asia since 800 CE. *Clim Dyn* 41(11–12):2957–2972
- Duffresne J-L, Foujols M-A, Denvil S, Caubel A, Marti O, Aumont O, Balkanski Y, Bekki S, Bellenger H, Benshila R (2013) Climate change projections using the IPSL-CM5 Earth System Model: from CMIP3 to CMIP5. *Clim Dyn* 40(9–10):2123–2165
- Esper J, Schneider L, Krusic P, Luterbacher J, Büntgen U, Timonen M, Sirocko F, Zorita E (2013) European summer temperature response to annually dated volcanic eruptions over the past nine centuries. *Bull Volcanol* 75(7):1–14
- Ge QS, Zheng JY, Hao ZX, Shao XM, Wang W-C, Luterbacher J (2010) Temperature variation through 2000 years in China: an uncertainty analysis of reconstruction and regional difference. *Geophys Res Lett* 37, L03703. doi:10.1029/2009gl041281

- Ge Q, Zheng J, Hao Z, Liu H (2013) General characteristics of climate changes during the past 2000 years in China. *Sci China Earth Sci* 56(2):321–329
- Guiot J, Corona C, Escarsel (2010) Growing season temperatures in Europe and climate forcings over the past 1400 years. *PLoS ONE* 5:3. doi:10.1371/journal.pone.0009972
- Jones PD, Briffa KR, Barnett TP, Tett SFB (1998) High-resolution palaeoclimatic records for the last millennium: interpretation, integration and comparison with General Circulation Model control-run temperatures. *The Holocene* 8(4):455–471
- Jones PD, Lister DH, Osborn TJ, Harpham C, Salmon M, Morice CP (2012) Hemispheric and large-scale land-surface air temperature variations: an extensive revision and an update to 2010. *J Geophys Res* 117:D5. doi:10.1029/2011jd017139
- Jungclauss JH, Lorenz SJ, Timmreck C, Reick CH, Brovkin V, Six K, Segsneider J, Giorgetta MA, Crowley TJ, Pongratz J, Krivova NA, Vieira LE, Solanki SK, Klocke D, Botzet M, Esch M, Gayler V, Haak H, Raddatz TJ, Roeckner E, Schnur R, Widmann H, Claussen M, Stevens B, Marotzke J (2010) Climate and carbon-cycle variability over the last millennium. *Clim Past* 6(5):723–737
- Landrum L, Otto-Bliessner BL, Wahl ER, Conley A, Lawrence PJ, Rosenbloom N, Teng H (2013) Last millennium climate and its variability in CCSM4. *J Clim* 26(4):1085–1111
- Li J, Sun C, Jin F-F (2013) NAO implicated as a predictor of Northern Hemisphere mean temperature multidecadal variability. *Geophys Res Lett* 40:5497–5502
- Ljungqvist FC, Krusic PJ, Brattström G, Sundqvist HS (2012) Northern Hemisphere temperature patterns in the last 12 centuries. *Clim Past* 8(1):227–249
- Man W, Zhou T (2014) Regional-scale surface air temperature and East Asian summer monsoon changes during the last millennium simulated by the FGOALS-gl climate system model. *Adv Atmos Sci* 31(4):765–778
- Mann ME, Rutherford S, Wahl E, Ammann C (2007) Robustness of proxy-based climate field reconstruction methods. *J Geophys Res* 112, D12109. doi:10.1029/2006jd008272
- Mann ME, Zhang ZH, Hughes MK, Bradley RS, Miller SK, Rutherford S, Ni FB (2008) Proxy-based reconstructions of hemispheric and global surface temperature variations over the past two millennia. *Proc Natl Acad Sci U S A* 105(36):13252–13257
- Mann ME, Zhang ZH, Rutherford S, Bradley RS, Hughes MK, Shindell D, Ammann C, Faluvegi G, Ni FB (2009) Global signatures and dynamical origins of the Little Ice Age and Medieval Climate Anomaly. *Science* 326(5957):1256–1260
- Mann ME, Fuentes JD, Rutherford S (2012) Underestimation of volcanic cooling in tree-ring-based reconstructions of hemispheric temperatures. *Nat Geosci* 5(3):202–205
- Masson-Delmotte V, Schulz M, Abe-Ouchi A, Beer J, Ganopolski A, Rouco J, Jansen E, Lambeck K, Luterbacher J, Naish T (2013) Information from paleoclimate archives. In: Stocker TF et al (eds) *Climate change 2013: the Physical Science Basis. Contribution of Working Group I to the Fifth Assessment Report of the Intergovernmental Panel on Climate Change*. Cambridge Univ. Press, Cambridge
- Moberg A, Sonechkin DM, Holmgren K, Datsenko NM, Karlén W (2005) Highly variable Northern Hemisphere temperatures reconstructed from low- and high-resolution proxy data. *Nature* 433(7026):613–617
- Neukom R, Luterbacher J, Villalba R, Kuttel M, Frank D, Jones PD, Grosjean M, Wanner H, Aravena JC, Black DE, Christie DA, D'Arrigo R, Lara A, Morales M, Soliz-Gamboa C, Srur A, Urrutia R, von Gunten L (2011) Multiproxy summer and winter surface air temperature field reconstructions for southern South America covering the past centuries. *Clim Dyn* 37(1–2):35–51
- Newman L, Wanner H, Kiefer T (2009) Towards a global synthesis of the climate of the last 2 millennium. *PAGE S News* 17(3):130
- PAGES 2k Consortium (2013) Continental-scale temperature variability during the past two millennia. *Nat Geosci* 6(5):339–346
- Schmidt GA, Jungclauss JH, Ammann CM, Bard E, Braconnot P, Crowley TJ, Delaygue G, Joos F, Krivova NA, Muscheler R, Otto-Bliessner BL, Pongratz J, Shindell DT, Solanki SK, Steinhilber F, Vieira LEA (2012) Climate forcing reconstructions for use in PMIP simulations of the Last Millennium (v1.1). *Geosci Model Dev* 5(1):185–191
- Schmidt GA, Kelley M, Nazarenko L, Ruedy R, Russell GL, Aleinov I, Bauer M, Bauer SE, Bhat MK, Bleck R (2014) Configuration and assessment of the GISS ModelE2 contributions to the CMIP5 archive. *J Adv Model Earth Syst* 6(1):141–184
- Schneider, T (2001) Analysis of incomplete climate data: Estimation of mean values and covariance matrices and imputation of missing values. *J Clim* 14(5): 853–871
- Schurer A, Hegerl G, Mann ME, Tett SFB, Phipps SJ (2013) Separating forced from chaotic climate variability over the past millennium. *J Clim* 26(18):6954–6973

- Shi F, Yang B, von Gunten L (2012) Preliminary multiproxy surface air temperature field reconstruction for China over the past millennium. *Sci China Earth Sci* 55(12):2058–2067
- Timmreck C, Lorenz SJ, Crowley TJ, Kinne S, Raddatz TJ, Thomas MA, Jungclaus JH (2009) Limited temperature response to the very large AD 1258 volcanic eruption. *Geophys Res Lett* 36. doi:10.1029/2009gl040083
- Wang S, Wang R (1990) Seasonal and annual temperature variations since 1470 AD in East China. *Acta Meteorol Sin* 4(3):428–439
- Wang S, Wen X, Luo Y, Dong W, Zhao Z, Yang B (2007) Reconstruction of temperature series of China for the last 1000 years. *Chin Sci Bull* 52(23):3272–3280
- Wang J, Emile-Geay J, Guillot D, Smerdon JE, Rajaratnam B (2014) Evaluating climate field reconstruction techniques using improved emulations of real-world conditions. *Clim Past* 10(1):1–19
- Wu T, Yu R, Zhang F, Wang Z, Dong M, Wang L, Jin X, Chen D, Li L (2010) The Beijing Climate Center atmospheric general circulation model: description and its performance for the present-day climate. *Clim Dyn* 34(1):123–147
- Wu G, Liu Y, He B, Bao Q, Duan A, Jin F-F (2012) Thermal controls on the Asian summer monsoon. *Sci. Rep.*, 2, 404. doi:10.1038/srep00404
- Yang F, Shi F, Kang S, Wang S, Xiao Z, Nakatsuka T, Shi J (2013) Comparison of the dryness/wetness index in China with the Monsoon Asia Drought Atlas. *Theor Appl Climatol* 114(3–4):553–566
- Zhang D (1980) Winter temperature changes during the last 500 years in South China. *Chin Sci Bull* 25(6): 497–500